2013

Raman scattering studies of strain effects in (100) and (311)B GaAs 1-xBix epitaxial layers

J A. Steele
University of Wollongong, js598@uowmail.edu.au

Roger A. Lewis
University of Wollongong, roger@uow.edu.au

M Henini
University of Nottingham

O M. Lemine
Al Imam Muhammad Ibn Saud Islamic University (IMSIU)

A Alkaoud
Al Imam Muhammad Ibn Saud Islamic University (IMSIU)

Raman scattering studies of strain effects in (100) and (311)B GaAs 1-xBix epitaxial layers

Abstract

We report room-temperature Raman studies of strained (100) and (311)B GaAs1-xBix epitaxial layers for x ≤ 0.039. The Raman spectra exhibit a two-mode behavior, as well as disorder-activated GaAs-like phonons. The experimental results show that the GaAs-like LO(Γ) mode experiences a strong composition-dependent redshift as a result of alloying. The peak frequency decreases linearly from the value for pure GaAs (∼293 cm-1) with the alloyed Bi fraction x and the introduced in-plane lattice strain ε, by Δ ω LO = Δ ω alloy-Δ ω strain. X-ray diffraction measurements are used to determine x and ε allowing Δ ω alloy to be decoupled and is estimated to be-12(±4) cm-1/x for (100) GaAs1- xBix. Δ ω LO is measured to be roughly double for samples grown on (311)B-oriented substrates to that of (100) GaAs. This large difference in redshift is accounted for by examining the Bi induced strain, effects from alloying, and defects formed during high-index (311)B crystal growth.

Keywords

epitaxial, strain, raman, studies, xbix, 1, gaas, b, 311, 100, effects, layers, scattering

Disciplines

Engineering | Physical Sciences and Mathematics

Publication Details

Steele, J. A., Lewis, R. A., Henini, M., Lemine, O. M. & Alkaoud, A. (2013). Raman scattering studies of strain effects in (100) and (311)B GaAs 1-xBix epitaxial layers. Journal of Applied Physics, 114 (19), 193516-1-193516-6.

Raman scattering studies of strain effects in (100) and (311)B $GaAs_{1-x}Bi_x$ epitaxial layers

J. A. Steele,[1,a)] R. A. Lewis,[1] M. Henini,[2] O. M. Lemine,[3] and A. Alkaoud[3]
[1]*Institute for Superconducting and Electronic Materials, University of Wollongong, Wollongong, NSW 2522, Australia*
[2]*School of Physics and Astronomy, Nottingham Nanotechnology and Nanoscience Center, University of Nottingham, Nottingham NG7 2RD, United Kingdom*
[3]*Department of Physics, College of Sciences, Al Imam Muhammad Ibn Saud Islamic University (IMSIU), Riyadh, 11623, Saudi Arabia*

(Received 18 August 2013; accepted 3 November 2013; published online 21 November 2013)

We report room-temperature Raman studies of strained (100) and (311)B $GaAs_{1-x}Bi_x$ epitaxial layers for $x \leq 0.039$. The Raman spectra exhibit a two-mode behavior, as well as disorder-activated GaAs-like phonons. The experimental results show that the GaAs-like LO(Γ) mode experiences a strong composition-dependent redshift as a result of alloying. The peak frequency decreases linearly from the value for pure GaAs ($\sim 293\,cm^{-1}$) with the alloyed Bi fraction x and the introduced in-plane lattice strain $\varepsilon_{\|}$, by $\Delta\omega_{LO} = \Delta\omega_{alloy} - \Delta\omega_{strain}$. X-ray diffraction measurements are used to determine x and $\varepsilon_{\|}$ allowing $\Delta\omega_{alloy}$ to be decoupled and is estimated to be $-12(\pm 4)$ cm^{-1}/x for (100) $GaAs_{1-x}Bi_x$. $\Delta\omega_{LO}$ is measured to be roughly double for samples grown on (311)B-oriented substrates to that of (100) GaAs. This large difference in redshift is accounted for by examining the Bi induced strain, effects from alloying, and defects formed during high-index (311)B crystal growth. © *2013 AIP Publishing LLC*. [http://dx.doi.org/10.1063/1.4831947]

I. INTRODUCTION

GaAsBi is an important III-V-bismide ternary alloy receiving much current attention, not only for its promising physical properties but also in methods of increasing the Bi solubility.[1–7] This is because growers are currently confronted with some physical and technical issues that have thus far restricted the amount of Bi able to be introduced into the GaAs matrix.[8] The largest Bi incorporation experimentally reported has been $x = 0.22$ for $GaAs_{1-x}Bi_x$ films grown on bulk (100) GaAs substrate.[9] Recently, high-index (311)B-oriented substrates were shown to allow for a sizably larger Bi incorporation at stoichiometric conditions to that of (100) GaAs.[1] These results present a potential approach to improving the Bi incorporation efficiency in (In)GaAsBi(N) materials, for long-wave device applications,[10] through adopting high-index substrates such as (311)B. Thus, it is important to first investigate the constituent alloy GaAsBi for its optical, vibrational, and electronic properties. The same samples investigated in Ref. 1 are studied in this paper.

When a bismuth atom substitutionally replaces an As atom in a GaAs crystal, lattice deformation and new vibrational modes localized around the bismuth atom are produced. Raman and resonant Raman spectroscopy have proven extremely successful in investigating the electronic and vibrational properties of the now relatively well-studied GaAs(N, P, Sb) alloys. We find, however, only two Raman studies of GaAsBi epitaxial alloys in the literature.[11,12] Both studies set out to identify new GaBi modes, each focusing on two (100) GaAsBi samples of relatively low bismuth concentrations ($x \leq 0.024$ (Ref. 11) and $x \leq 0.031$ (Ref. 12)). This highlights the need for further investigations of GaAsBi. The relatively large difference in electronegativity and lattice parameter of GaBi (12%) and GaN (20%) to that of GaAs make these alloys scientifically interesting. As a consequence, alloying introduces biaxial strain which has dramatic effects on Raman spectra (RS). Both GaAsN and GaAsBi exhibit a two-mode behavior, consistent with our current study. We show here both also display similar disorder-activated GaAs-type bands, thus, it is particularly useful here to make the comparison. In this study, we focus on the GaAs-like LO(Γ) mode evolution with increasing bismuth content for samples grown on (100) and (311)B substrates.

II. EXPERIMENT

The alloys were grown by molecular-beam epitaxy with varying Bi concentrations in the range of $0.012 \leq x \leq 0.039$. The nominal thickness of the $GaAs_{1-x}Bi_x$ epilayers is $\sim 1\,\mu m$. The coherent, tensile strain in the epilayers was confirmed by X-ray diffraction (XRD) measurements and our RS. Bismuth contents were determined using XRD by assessing the Bragg angle of the GaAs and GaAsBi reflections.[9,13] Asymmetric reciprocal space maps (not shown) revealed that the epilayers were grown coherently on both (100) and (311)B GaAs substrates, such that the degree of plastic relaxation in all the samples is close to zero. Further details of the sample preparation and characterization are given elsewhere.[1]

Room temperature Raman spectra were acquired using a Jobin-Yvon HR800 integrated Raman system employing an Olympus 100× microscope, a 20 mW HeNe laser working at 632.81 nm, and an air-cooled CCD detector. RS were dispersed using an 1800 g/mm diffraction grating and correct

a)Electronic mail: js598@uowmail.edu.au

instrument calibration was verified by checking the position of the Si band at $\pm 520.7\,\mathrm{cm}^{-1}$. With the addition of two linear polarizers, measurements were performed in a quasi-backscattering experimental configuration (described as $-c(\vec{E}_{incident}, \vec{E}_{scattered})c$ in Porto notation[14]). For our samples, the epilayer thicknesses are large compared to $d_{opt} = 1/(2\alpha)$,[15] so that there is negligible signal from the substrate. The beam was focused using the micro-Raman setup, allowing for spectra mapping on multiple points on the sample surface with a probe spatial resolution of $\sim 2\,\mu$m and spectral resolution of $0.2\,\mathrm{cm}^{-1}$. Such measurements indicated the samples were highly homogeneous with respect to phonon frequencies and the general Raman lineshape.

III. RESULTS

A. XRD characterization

XRD scans reported in Fig. 1 of Ref. 1 (performed in 2007) have been compared to measurements performed 6 years later (Fig. 1). No notable changes or signs of degradation are observed. Moreover, Energy-dispersive X-ray spectroscopy (EDS) measurements performed on all samples ensured no oxidation or other degrading chemical changes occurred on their surfaces during this time.

For sample grown on (100) and (311)B GaAs, the (400) and (311) symmetrical reflections were measured, respectively, using an X-ray wavelength of $\lambda = 1.54\,\text{Å}(\mathrm{Cu}K_{\alpha_1})$. Figure 1 shows measured XRD data for the near-stoichiometric GaAsBi samples grown on (100) and (311)B GaAs, with controls ($x = 0$) also displayed for comparison. Similar curves were recorded for the rest of the samples. From these data, the lattice distortions $\Delta d/d$, defined as the relative change of the distance between lattice planes, can be calculated from the relation $\Delta d/d = \cot\theta(\Delta\theta)$, where θ is the Bragg angle for the GaAs substrate reflections and $\Delta\theta$ is the angular shift of the GaAsBi

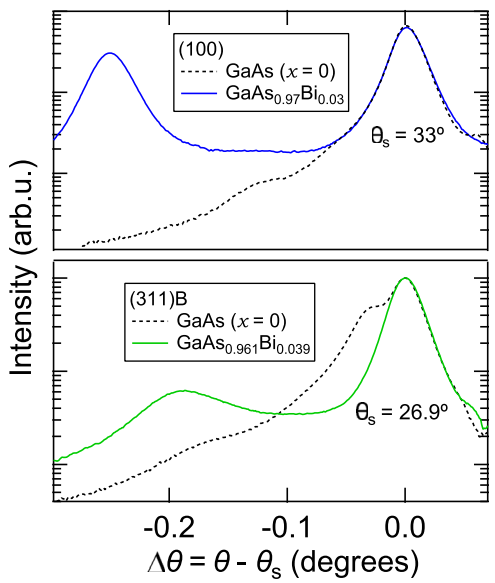

FIG. 1. Comparison of measured XRD scans from symmetric (113) and (004) Bragg reflections for as-grown GaAs (dotted lines) and near-stoichiometric $GaAs_{1-x}Bi_x$ (solid lines) epilayers grown on (100) and (311)B GaAs substrates. θ_s represents the Bragg angle of reflection for the GaAs substrates.

epilayer reflections with respect to the GaAs substrate. From the experimental determination of $\Delta d/d$, we can calculate the relaxed lattice parameter of the GaAsBi films by

$$a_{\mathrm{rel}} = a_{\mathrm{GaAs}}[1 + P(\Delta d/d)]. \tag{1}$$

For both orientations, we observe a linear increase of $(a_{\mathrm{rel}} - a_{\mathrm{GaAs}})$ with Bi concentration

$$x = \left(\frac{a_{\mathrm{GaAs}}}{a_{\mathrm{GaBi}} - a_{\mathrm{GaAs}}}\right) P(\Delta d/d). \tag{2}$$

Here, parameter P is the distortion coefficient of the GaAsBi films, which is dependent on the elastic constants of GaAs and samples orientation. The parameters a_{GaAs} and a_{GaBi} represents the lattice constant of GaAs (5.65 Å) and GaBi (6.33 Å, Ref. 13), respectively. Given that the Bi content of our samples is quite low, we estimate values for P using the elastic parameter of pure GaAs such that $P_{100} = 0.527$ and $P_{311} = 0.691$ (an in-depth discussion on (N11)-oriented films can be found elsewhere[16]). Regardless of growth direction, the in-plane strain (lattice mismatch) is given by

$$\epsilon_{\parallel} = \frac{(a_{\mathrm{rel}} - a_{\mathrm{GaAs}})}{a_{\mathrm{GaAs}}}. \tag{3}$$

In Fig. 1, we see that the XRD shapes for $x = 0$ strongly differ for the two orientations. There is a small peak appearing at a slightly lower reflection angle for the (311)B GaAs control epilayer. Such XRD lineshapes have been previously observed for (311)A and (311)B GaAs epilayers being attributed to excess As as a consequence of varying the growth temperatures and/or V:III flux ratios.[17,18] The mechanisms leading to an enhanced concentration of As_{Ga} in (311)B GaAs and the effect it has on the RS are discussed later in detail.

The epilayer XRD peak is seen to be broader in (311)B-oriented GaAsBi samples. In fact, the FWHM of (311)B epilayers was found to increase with rising Bi concentrations, whereas only an initial widening was seen for samples grown on (100) substrates. This suggests the quality of the (311)B $GaAs_{1-x}Bi_x$ epilayers is poor, possessing a substantial degree of structural disorder. It is worth noting that while the intensity and width of the substrate reflections are comparable for both orientations, a much smaller relative intensity is observed from the (311)B $GaAs_{1-x}Bi_x$ epilayers. This indicates an appreciably thinner epilayer resulting from a slower growth rate in the (311)B direction.

In Table I, results of sample characterization for all samples are displayed. X-ray diffraction measurements of epilayer lattice constants are widely used to determine the Bi content of $GaAs_{1-x}Bi_x$ epilayers through the proportionality of a_{rel} and GaBi molar fraction.[2,6,9] The rate of change of the $x(\Delta d/d)$ for (100)- and (311)B-oriented epilayers differ greatly. This is simply a consequence of the difference in Bragg reflection angle and P value used for corresponding calculations.

The EDS modality does not lend itself to the absolute determinations of composition in thin semiconductor epitaxial

TABLE I. List of samples studied in this work with results from epilayer characterization. The numbers in parentheses represent the uncertainty for Bi content x in units of the last significant digits. Results from standardless EDS measurements are presented for comparison showing relative changes in Bi content, with an uncertainty of ±2.0 (rel.) for each.

Sample	$\lvert\Delta\theta\rvert$ (deg)	$\Delta d/d$ ($\times 10^{-3}$)	$\epsilon_{\parallel}$ ($\times 10^{-3}$)	$x_{(XRD)}$ (%)	$x_{(EDS)}$ (rel.)
		(100)-oriented			
1[a]	0	0	0	0	0
2	0.15	4.1	2.1	1.8(3)	2.2
3	0.23	6.2	3.3	2.7(2)	2.5
4	0.25	6.8	3.6	3.0(3)	3.0
		(311)B-oriented			
5[a]	0.025	0.85	0.58	NA	0
6	0.060	2.0	1.4	1.2(1)	2.2
7	0.16	5.7	3.9	3.3(3)	3.1
8	0.17	6.1	4.2	3.5(2)	3.1
9	0.19	6.8	4.7	3.9(2)	3.6

[a]Control samples ($x = 0$) grown for both substrate orientations.

layers, as it usually involves significant components of scaling and relative error. However, we use standardless EDS quantitative analysis (see Table I) to confirm the relative increase of Bi incorporation between samples. To permit better comparison with the XRD data, the EDS data were scaled such that a linear fit of $x_{EDS}(x_{XRD})$ has a gradient of one. We see a steady correlative rise in Bi composition for the two methods. For the completeness of later discussion, the small peak appearing in the XRD scan of the (311)B GaAs control ($x = 0$) has been added.

B. Raman scattering measurements

1. Disorder-activated GaAs-like modes

Figure 2 displays the typical RS of near-stoichiometric (100) $GaAs_{1-x}Bi_x$ ($x = 0.030$) exhibiting the two-mode behavior. Data for both $-z(Y, Y)z$ and $-z(x, y)z$ quasi-backscattering geometries are shown. Here, z and $-z$ represent the incident and scattered photon directions (001) and $(00\bar{1})$, while $x = (100)$, $y = (010)$, and $Y = (110)$. According to the Raman selection rules in a zincblende crystal (T_d site symmetry), the LO(Γ) phonon is allowed, however, the TO(Γ) is forbidden in these scattering geometries. The appearance of TO(Γ) as a dominant feature of the RS in Fig. 2 can be attributed to bismuth-induced disorder in the lattice, resulting in a relaxation of the Raman selection rules. Just below the GaAs-like TO peak appears a broad feature which is assigned to a disorder-activated TO (DATO) mode. Likewise, in the spectral range from 65 cm^{-1} to 200 cm^{-1}, weak disorder-activated transverse acoustic (DATA) and disorder-activated longitudinal acoustic (DALA) bands (as confirmed by $-z(x, x)z$ spectra which are not shown) are observed together with second-order Raman signatures of acoustic phonons. These disorder-activated modes are observed for both (100) and (311)B growth directions and indicate large lattice deformation effects. The most prominent of these features is the 2TA(X) mode at ~160 cm^{-1}. The small feature at ~200 cm^{-1} was clearly observed in most RS of both (100) and (311)B-oriented samples with relatively large Bi concentration. TA(X) + 2TA(L) possess the only adequate Raman shift and thus was attributed to this higher-scattering combination, although further investigations are required to confirm this.

Strong features at ~228 cm^{-1} and ~240 cm^{-1}, which have been observed in previous GaAsBi Raman studies[12] are GaAs-like LA(X) and LO(L) phonons, respectively. In the first-order Raman scattering, these zone-boundary phonons are forbidden in pristine GaAs because of momentum conservation. These features have been observed in Raman studies of strained GaAsN,[19,20] where the activation of the zone-boundary phonons is attributed to the nitrogen-induced mixing of the GaAs conduction bands.[21] Similar to the nitridation of GaAs, the incorporation of Bi into GaAs is also expected to cause a mixing of the GaAs valence bands.[12] We clearly see the two previously discovered GaBi-like modes at ~185 cm^{-1} and ~213 cm^{-1}, which have been identified theoretically[4] as TO(Γ) and LO(Γ) phonons, respectively. The mode at ~140 cm^{-1}, labeled Bi_x, is of unclear origin as no single or combination of GaAs-like phonon modes can be used to explain its appearance. We simply acknowledge it here as it appears in the RS of our samples and is also reported by Verma *et al.*[11] The frequency of the GaBi-like phonons do *not* appear to shift over this compositional range, however, clearly strengthens with increasing Bi concentration. If there was only a very slight shift, accurate frequency determination is made difficult by the superposition of the various disorder-activated modes. A more comprehensive examination into the behavior of these modes is currently under way for an extended Bi compositional range.

2. GaAs-like optical modes

Next, we carry out a detailed analysis of the frequency behavior of the GaAs-like optical phonons for varying Bi incorporation for both (100) and (311)B growth directions. Phonon frequencies are strongly dependent on any strain

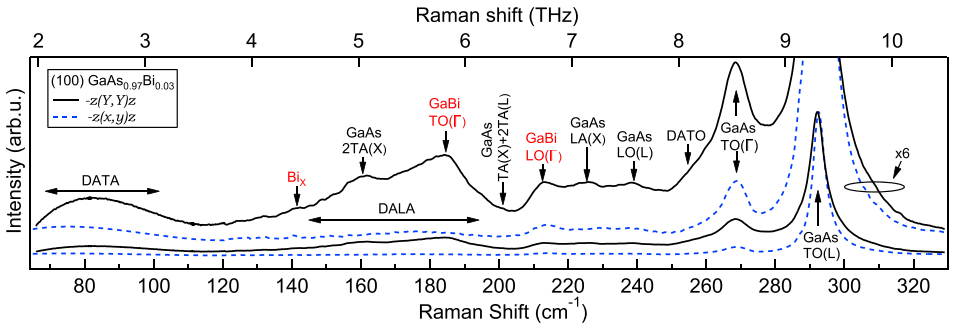

FIG. 2. Room-temperature RS of near-stoichiometric (100) $GaAs_{1-x}Bi_x$ ($x = 0.030$) in $-z(Y, Y)z$, solid line, and $-z(x,y)z$, dashed line, quasi-backscattering geometries. To reveal weaker features, the upper traces have been reproduced enlarged six times and offset.

present in the GaAs-based alloys.[22–26] Such stress-induced shifts can be essentially explained by the phonon deformation potentials (PDPs). Detailed expressions for PDPs and their consequences for the first-order Raman shifts are well summarized by Adachi.[27]

Due to the disorder-induced break down of the selection rules, the forbidden TO(Γ) mode is enhanced in the RS allowing unambiguous frequency determination. The absence of the lattice relaxation (or the preservation of the in-plane substrate lattice constant) in the $GaAs_{x-1}Bi_x$ epilayers manifests itself by a very weak dependence on the Bi content. We thus see the biaxial strain having a significant effect on the LO(Γ) phonon frequency. Figure 3 shows a comparison of the redshift in the GaAsBi samples for both (100) and (311)B orientations, for the given Bi concentrations. With even only a small amount of Bi introduced, the GaAs-like LO(Γ) phonon mode softens to lower frequencies. A comparable redshift is experienced for both sample orientations in Fig. 3, even though the Bi content of the (311)B sample is less than half that of the (100) sample.

We plot in Fig. 4 the frequency of the LO(Γ) versus Bi content x for all samples. The figure shows a distinct shift towards lower energies and broadens with increasing x in the epilayers. We define the frequency redshift as the difference in peak position between the $GaAs_{1-x}Bi_x$ epilayer and bulk GaAs; $\Delta\omega_{LO} = \omega_{LO} - \omega^0_{LO}$, where ω_{LO} and ω^0_{LO} are the measured vibration frequencies for our $GaAs_{1-x}Bi_x$ epilayers and for pristine GaAs, respectively. Although conventionally quadratic equations are used to describe the frequency variations with x in III-V alloys,[28] the small range (with respect to GaAsSb or GaAsN) of x we present here warrants only a linear fit. From a linear fit of these data, we obtain the following composition dependence from the GaAs-like LO(Γ) mode in stressed (100) and (311)B $GaAs_{1-x}Bi_x$:

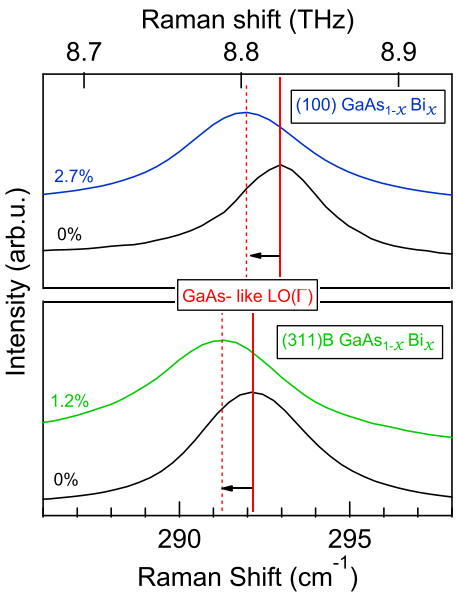

FIG. 3. Normalized room-temperature RS of (100) and (311)B $GaAs_{1-x}Bi_x$ epilayers in $-z(Y, Y)z$ geometry over the GaAs-like LO(Γ) energy range. The redshifts here are comparable for both (100) and (311)B crystal growth orientations, with Bi contents of $x = 0.027$ and $x = 0.012$, respectively.

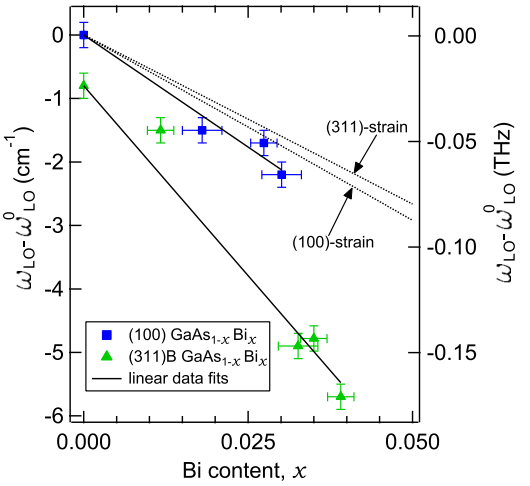

FIG. 4. Frequency of the GaAs-like LO(Γ) modes obtained from the RS of our (100) and (311)B $GaAs_{1-x}Bi_x$ epilayers with their linear fits displayed as solid lines. The two dashed lines labeled "strain" is the expected effect of strain only in both (100) and (311)B crystal orientations.

$$\omega_{LO}(\mathrm{cm}^{-1}) = \omega^0_{LO} + \Delta\omega_{LO}^{(100),\,(311)\mathrm{B}} \times x, \tag{4}$$

where the measured redshift values are $\Delta\omega_{LO}^{(100)} = -71(\pm 4)$ cm^{-1} and $\Delta\omega_{LO}^{(311)} = -120(\pm 6)\,\mathrm{cm}^{-1}$. The observed slope of the $GaAs_{1-x}Bi_x$ data will have a significant contribution from the effects of strain, as well as smaller effects due to alloying (the substitutional replacement of As atoms with Bi). The total redshift term can then be expressed as

$$\Delta\omega_{LO} = \Delta\omega_{alloy} - \Delta\omega_{strain}. \tag{5}$$

For the biaxial strain component, the size of the shift is linearly dependent on the in-plane strain (Eq. (3)). Assuming the deformation constants of $GaAs_{1-x}Bi_x$, for $x \leq 0.039$, are the same as those for pure GaAs, and applying Vegard's law, we obtain an estimation of strain only LO(Γ) shift using the methods prescribed by Cerdeira *et al.*[23] The strain only redshift estimated for the (100)-oriented samples is $\Delta\omega_{strain} = -59\,\mathrm{cm}^{-1}/x$. This is compared to our measured total redshift of $-71(\pm 4)$ cm^{-1}/x. The additional redshift component may be attributable to the effects of alloying, whereby the total number of Ga-As bonds is reduced, such that $\Delta\omega_{alloy} = -12(\pm 4)\,\mathrm{cm}^{-1}$. This value for alloying shift is rather low when compared to the alloying effects observed for $GaAs_{1-x}N_x$ (Refs. 22 and 29) ($\sim 40\,\mathrm{cm}^{-1}/x$) and considering most of the alloying-induced shift in the phonon bands is experienced in the dilute range. Further measurements on fully relaxed $GaAs_{1-x}Bi_x$ would aid comparison.

It is notable that for the (311)B GaAs ($x = 0$) the LO(Γ) mode is dampened by $\sim 0.7\,\mathrm{cm}^{-1}$. This frequency shift was verified through mapping of large areas of the epilayer surface of the control. The samples were grown at near-stoichiometric conditions (i.e., when As flux is nearly the same as Ga flux) in order to incorporate Bi. As discussed in the XRD characterization, this large shift in frequency for the control arises due to an increased number of As antisite (As_{Ga}) defects inherent in high-index (311)B GaAs epitaxial growth. The strain determined from the small offset in the

XRD scans (0.58×10^{-3}) is less than 1/3 of that required (1.8×10^{-3}) to cause a redshift of $\sim 7\,\mathrm{cm}^{-1}$. Therefore, strain caused by the presence of As antisites cannot explain the entire shift. The FWHM of the LO phonon peak for (100) GaAs and (311)B GaAs control epilayers are $2.7\,\mathrm{cm}^{-1}$ and $3.8\,\mathrm{cm}^{-1}$, respectively, further indicating an inferior structural quality in the latter.

It is interesting that the contribution of strain only effects in the (311) surfaces are predicted to be less to that of (100)-oriented samples (see Fig. 4). The total rate of redshift measured here for the (311)B $GaAs_{1-x}Bi_x$ samples is $\Delta\omega_{LO} = -120(\pm 6)\,\mathrm{cm}^{-1}/x$, which is relatively large. Evoking the concept of "phonon confinement," the enhanced LO(Γ) phonon redshift arises from increased crystal defects inherent to (311)B crystal growth. Phonon confinement can cause optical phonons to redshift frequency, broaden and even become asymmetric. This occurs because the phonon, confined in direct space within a sphere of diameter L, can be described in reciprocal space by a wave packet with a range of k-values, $\Delta k \approx L^{-1}$.[30] Thus, the response observed in the RS is governed by a convolution of the ω vs. k phonon dispersion and the wave packet. Tiong *et al.*[31] employed the phonon confinement model to interpret the LO(Γ) phonon shift caused by bombardment of (100) GaAs with 270 keV As^+ ions, and its dependence on fluence. They[31] observed a maximum induced redshift before the LO(Γ) peak broadened into a continuum. RS of this kind is indicative of amorphous GaAs, in which the crystal begins to lack long-range order.

The (311) GaAs(Bi) surface contains equal number of (100)-like atoms having two surface-dangling bonds and (111)-like atoms having one surface-dangling bond. A type-A surface contains (100) As(Bi) atoms and (111)A-like Ga atoms, while a type-B surface contains (100)-like Ga atoms and (111)B-like As(Bi) atoms. It has been explained[32] that a (N11)A surface has very low affinity for impurities and defect incorporation, when compared to the (N11)B surface, since its dangling bond is empty. However, in (N11)B surfaces, the two unbonded valence electrons of the As(Bi) atoms become very reactive. While Bi incorporation is ultimately enhanced, this makes (311)B growth prone to impurities and defects. Invoking the notion, an increase in defect density is the cause to the large dampening is supported by Fig. 1 from Ref. 1, which shows transmission electron microscopy (TEM) images for (100) and (311)B GaAsBi samples grown at near-stoichiometric conditions. These images reveal the presence of extended structural defects in both layers. In the case of (100) GaAsBi film, such defects consist mainly of dislocations. However, for the (311)B sample, the crystalline quality is shown to be fairly good at the growth interface where microtwins are observed, but degrades heavily near the surface. Z-contrast imaging also shows no Bi segregation near the GaAsBi/GaAs interface, despite the large amount of disorder. Coupled with the homogeneous surface mapping of RS, the increased redshift in (311)B samples cannot be explained by Bi clustering. Thus, the clear correlative behavior of the LO(Γ) redshifted frequency and the Bi concentration x, for samples grown on a (311)B-oriented substrate, presumably arises from confinement of the phonon in the defective GaAsBi matrix.

Strong dampening effects on the LO(Γ) mode of our (311)B GaAsBi samples can likely be avoided by crystal growth below the critical thickness where defects develop. Raman scattering studies only examine the vibration properties near the surface of solids, thus, one can only assume the enhanced redshift would not be observed near the epilayer interface where the crystal is coherently grown. While it is possible to improve the structural properties of these samples through optimizing growth conditions, we speculate that a more accurate Raman study would be achieved with thinner epilayers.

IV. CONCLUSION

We have studied the influence of bismuth incorporation on the RS of strained (100) and (311)B $GaAs_{1-x}Bi_x$, for $0.012 \leq x \leq 0.039$. The first-order RS displays a two-mode behavior as well clear disorder-activated GaAs-like bands arising from a large lattice deformation. This is not surprising, given the large differences in natural bond lengths for GaBi and GaAs. The introduction of Bi into GaAs is shown to redshift the LO(Γ) mode at a rate of $\Delta\omega_{LO} = -71(\pm 4)\ \mathrm{cm}^{-1}/x$ for samples grown on (100) GaAs substrates. Once effects due to biaxial strain are removed, we estimate the contribution to the total shift from alloying to be $\Delta\omega_{alloy} = -12(\pm 4)\ \mathrm{cm}^{-1}$. $GaAs_{1-x}Bi_x$ samples grown on (311)B GaAs substrates are reported to experience large dampening, $-120(\pm 6)\ \mathrm{cm}^{-1}/x$, nearly twice that of the (100) grown samples. This is contrary to expected strain only effects. XRD scans, RS, and TEM images reveal that large amounts of disorder in the GaAsBi matrix are the likely origin for the discrepancy.

ACKNOWLEDGMENTS

The authors thank the Australian Research Council for support. We acknowledge the contributions of S. Novikov in preparing the samples and the Australian National Fabrication Facility (ANFF) - Materials Node for their provision of research facilities. O. M. Lemine, A. Alkaoud, and M. Henini acknowledge King Abdul-Aziz City for Sciences and Technology (KACST) for financial support under the National Plan for Sciences and Technology program (NPST)-Project No. 11-NAN1793-08.

[1]M. Henini, J. Ibáñez, M. Schmidbauer, M. Shafi, S. V. Novikov, L. Turyanska, S. I. Molina, D. L. Sales, M. F. Chisholm, and J. Misiewicz, Appl. Phys. Lett. **91**, 251909 (2007).
[2]Z. Chine, H. Fitouri, I. Zaied, A. Rebey, and B. El Jani, J. Cryst. Growth **330**, 35 (2011).
[3]H. Achour, S. Louhibi, B. Amrani, A. Tebboune, and N. Sekkal, Superlattices Microstruct. **44**, 223 (2008).
[4]A. Belabbes, A. Zaoui, and M. Ferhat, J. Phys.: Condens. Matter **20**, 415221 (2008).
[5]R. B. Lewis, D. A. Beaton, X. Lu, and T. Tiedje, J. Cryst. Growth **311**, 1872 (2009).
[6]X. Lu, D. A. Beaton, R. B. Lewis, T. Tiedje, and M. B. Whitwick, Appl. Phys. Lett. **92**, 192110 (2008).
[7]X. Lu, D. A. Beaton, R. B. Lewis, T. Tiedje, and Y. Zhang, Appl. Phys. Lett. **95**, 041903 (2009).
[8]H. Jacobsen, B. Puchala, T. F. Kuech, and D. Morgan, Phys. Rev. B **86**, 085207 (2012).

[9]R. B. Lewis, M. Masnadi-Shirazi, and T. Tiedje, Appl. Phys. Lett. **101**, 082112 (2012).
[10]S. J. Sweeney and S. R. Jin, J. Appl. Phys. **113**, 043110 (2013).
[11]P. Verma, K. Oe, M. Yamada, H. Harima, M. Herms, and G. Irmer, J. Appl. Phys. **89**, 1657 (2001).
[12]M. J. Seong, S. Francoeur, S. Yoon, A. Mascarenhas, S. Tixier, M. Adamcyk, and T. Tiedje, Superlattices Microstruct. **37**, 394 (2005).
[13]S. Tixier, M. Adamcyk, T. Tiedje, S. Francoeur, A. Mascarenhas, P. Wei, and F. Schiettekatte, Appl. Phys. Lett. **82**, 2245 (2003).
[14]T. C. Damen, S. P. S. Porto, and B. Tell, Phys. Rev. **142**, 570 (1966).
[15]D. E. Aspnes and A. A. Studna, Phys. Rev. B **27**, 985 (1983).
[16]J. Ibáñez, R. Kudrawiec, J. Misiewicz, M. Schmidbauer, M. Henini and M. Hopkinson, J. Appl. Phys. **100**, 093522 (2006).
[17]S. O'Hagan and M. Missous, J. Appl. Phys. **82**, 2400 (1997).
[18]J. Daeubler, M. Glunk, W. Schoch, W. Limmer, and R. Sauer, Appl. Phys. Lett. **88**, 051904 (2006).
[19]A. Mascarenhas and M. J. Seong, Semicond. Sci. Technol. **17**, 823 (2002).
[20]A. M. Mintairov, P. A. Blagnov, V. G. Melehin, N. N. Faleev, J. L. Merz, Y. Qiu, S. A. Nikishin, and H. Temkin, Phys. Rev. B **56**, 15836 (1997).
[21]M. J. Seong, A. Mascarenhas, and J. F. Geisz, Appl. Phys. Lett. **79**, 1297 (2001).
[22]J. Ibáñez, E. Alarcón-Lladó, R. Cuscó, L. Artús, and M. Hopkinson, J. Appl. Phys. **102**, 013502 (2007).
[23]F. Cerdeira, C. J. Buchenauer, F. H. Pollak, and M. Cardona, Phys. Rev. B **5**, 580 (1972).
[24]C. K. Inoki, V. Lemos, F. Cerdeira, and C. Vásquez-López, J. Appl. Phys. **73**, 3266 (1993).
[25]G. Armelles, M. J. Sanjuán, L. González, and Y. González, Appl. Phys. Lett. **68**, 1805 (1996).
[26]D. Serries, M. Peter, N. Herres, K. Winkler, and J. Wagner, J. Appl. Phys. **87**, 8522 (2000).
[27]S. Adachi, *GaAs and Related Materials: Bulk Semiconducting and Superlattice Properties* (John Wiley & Sons, Ltd., 1994), p. 103.
[28]I. F. Chang and S. S. Mitra, Adv. Phys. **20**, 359 (1971).
[29]T. Prokofyeva, T. Sauncy, M. Seon, M. Holtz, Y. Qiu, S. Nikishin, and H. Temkin, Appl. Phys. Lett. **73**, 1409 (1998).
[30]H. Richter, Z. P. Wang, and L. Ley, Appl. Solid State Commun. **39**, 625 (1981).
[31]K. K. Tiong, P. M. Amirtharaj, F. H. Pollak, and D. E. Aspnes, Appl. Phys. Lett. **44**, 122 (1984).
[32]X. Li, W. I. Wang, A. Y. Cho, and D. L. Sivco, J. Vac. Sci. Technol. B **11**, 912 (1993).